ROCKY EJECTA CRATERS AS A PROXY FOR THE EVOLUTION OF REGOLITH ON MARS. A. Rajšić[1], A. Lagain[2], S. Anderson[2], M. Golombek[3], N. Warner[4], G. Carboni[2], B.C. Johnson[1,5], K. Miljković[2], G.K. Benedix[2]. [1]Department of Earth, Atmospheric and Planetary Sciences, Purdue University, West Lafayette, IND, USA, [2]Space Science and Technology Centre, School of Earth and Planetary Sciences, Curtin University, Perth, Western Australia, [3]Jet Propulsion Laboratory, California Institute of Technology, Pasadena, CA, USA, [4]Department of Geological Sciences, SUNY Geneseo, Geneseo, NY, USA, [5]Department of Physics and Astronomy, Purdue University, West Lafayette, Indiana, USA

Introduction: Impact gardening is one of the most common geological processes in the Solar System. On airless planetary bodies or bodies without a thick atmosphere, billions of years of meteoritic bombardment lead to the production of regolith on the surface [1]. Nevertheless, meteoroid impacts simultaneously produce regolith (via impact gardening) and destroy it (via compaction). On Mars, this unconsolidated surface layer is meters thick and covers most of the planet. It is considered to be formed by impact, aeolian, and mass wasting processes [e.g., 2]. Its thickness depends on various geological processes, including erosion and deposition, but also on the topography and regolith maturity [3]. Recent results from the InSight mission have shown that the regolith layer is a dominantly impact-generated, sandy layer over Amazonian-Hesperian basalts that is meters thick [4] and consumes a significant portion of the kinetic energy of impacts affecting the number of detected impacts per martian year [5-8].

Different studies relate regolith production with impacts on the Moon [9-10]. Recent work on Mars focused on the InSight landing site as a type area for Hesperian to Early Amazonian lava plains on Mars [e.g., 11-12]. Comparison with another area [7] showed that local regolith thickness in the Late Amazonian volcanic unit is two times thinner than those measured at the InSight landing site (Early Amazonian-Hesperian). In this study, we estimate martian regolith thickness across different geological units to investigate the temporal dependency on regolith production.

Methodology: Rocky Ejecta Craters (REC) are simple craters characterized by boulders in the ejecta and have been used to estimate regolith thickness [e.g., 11] (Fig.1a). Although the abundance of boulders in the ejecta reflects the excavation of a strong bedrock material, the observation of small fresh craters with a complete lack of such rocky deposits surrounding them (Fresh Non-RECs (FNRECs)) is a diagnostic feature of an impact into poorly consolidated materials (i.e., regolith) [e.g., 11] (Fig.1b).

The survey and size measurement of both crater types was conducted using HiRISE images at 0.5 m/pixel. The initial crater population visible on an image was extracted using the Crater Detection Algorithm (CDA), a Convolutional Neural Network [13] trained on HiRISE imagery [14-15]. The CDA was applied on 14 HiRISE images (Fig.2) in geological units mapped as Late Amazonian (lAv) (2), Late (3) and Early Hesperian (lHvf, lHv, eHv) (3), Late (2), Middle (2), and Early Noachian (lNh, mNh, eNh) (2) [16]. Detected craters were between 5 m and 1.5 km in diameter and were subsequently sorted into REC and FNREC categories using a modified user interface from [17-18], employing a tkinter python module [18].

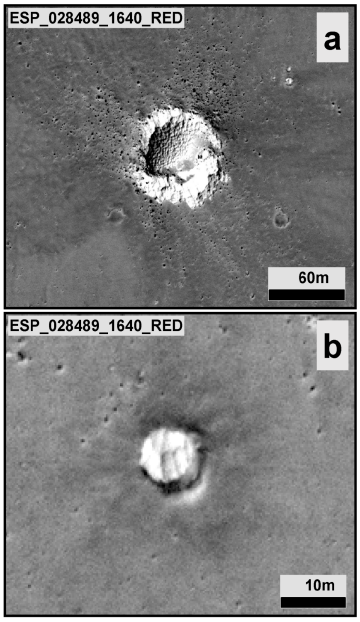

Figure 1. Example of a 60 m REC (a) and a 10 m FNREC (b) identified on ESP_28480_1640_RED HiRISE image.

Each HiRISE image was then manually surveyed a second time at a 1:4000 scale using ESRI's ArcMap software. Any missing RECs and FNRECs were identified and added to the database previously obtained. All craters of interest were finally measured using the CraterTools software [20], resulting in 257 RECs and 167 FNRECs. Model age for each region was derived using the Mars Crater Database from [21], CraterStatsII software [22], and the chronology from [23]. Model ages were inferred from craters larger than 1 km in diameter. Resurfacing events throughout geological history affect regolith thickness and the density of small craters. Here, we assume that the present-day regolith has been developed since the latest volcanic resurfacing event. So, model ages estimated by fitting the CSFD to the smallest crater population

represent the time over which observed regolith layers formed.

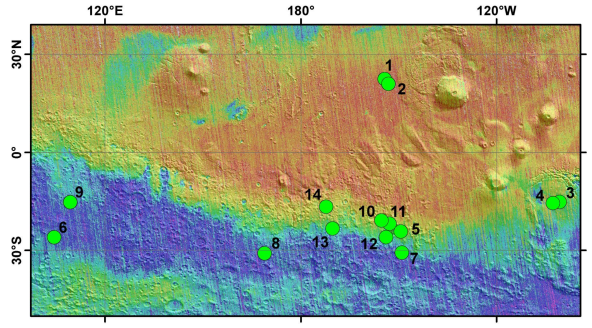

Figure 2. Location of surveyed areas. Background: TES dust cover index over MOLA shaded relief.

Results and Discussion: The regolith depth varies over very short distances due to the processes involved in its formation and the original geology and topography. Thus, simple crater size varies at a local scale. To mitigate this issue and assess the regolith thickness at a regional scale, we computed the median size of both crater types [10]. The average of the REC and FNREC median sizes provides a conservative threshold crater size from which the regolith depth can be inferred (black squares, Fig.3). Regolith thickness (Fig.3) was derived using the assumption that the depth of excavation in small craters is 0.084*x*D (D-crater diameter) [11, 12, 24].

Our results show that the depth of regolith on Amazonian and Hesperian terrain does not exceed ~3 m on average (horizontal dashed line, Fig.3). This is consistent with the regolith thickness reported by [12, 25] at the InSight landing site, where an Early Amazonian resurfacing episode of 1.7 Ga was inferred from craters <2 km in diameter. However, a detailed examination of local geology and boulder degradation [e.g., 26] is required to explain unexpectedly large REC craters mapped in Amazonian (labels 1, 2 in Fig.2, positive error bars Fig.3). We found that the regolith on terrains older than ~3.6 Ga is thicker than in younger units, with the average between ~5 and ~11 m. This correlates with the higher impact rate during the Noachian period, which resulted in thicker regolith in older units.

Conclusion: Automatic detection enabled the survey of a large number of craters in a short time. One of the perspectives of this study is scaling the experiment to numerous HiRISE images covering a wider variety of martian regions via retraining our algorithm to distinguish both classes of craters. Preliminary results show a sharp increase in regolith thickness between the Hesperian and Noachian periods, which is consistent with the primary process that controls regolith formation and thickness: the impact cratering rate. So, the total budget of regolith (destruction vs. creation) is positive at the geological timescale. Future work will consider estimating the effects of lower impact rates on the regolith compaction, as well as the role of local geology on the bedrock excavation and boulder erosion rate [26-27].

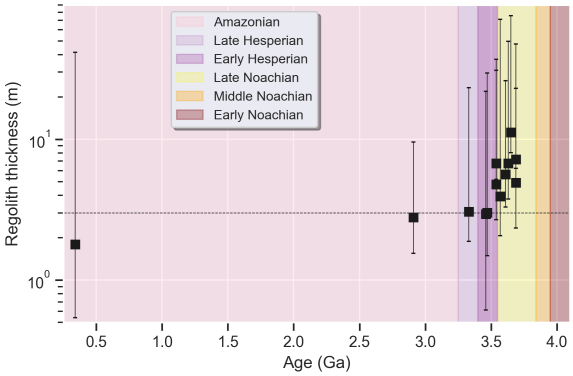

Figure 3. Threshold crater diameters (squares) are calculated from the average median size of both crater types measured in each region. Negative error bars on the threshold crater diameter correspond to the maximum size of FNRECs, while positive ones are the maximum size of RECs. The regolith thickness is assumed to be 0.084*x*D [23]. The dashed horizontal line marks the average regolith thickness (~3 m) in the Amazonian and Hesperian terrains.

References:

[1] Shoemaker, E.M. et al. (1969) *JGR* 74, 6081-6119. [2] Christensen P. & Moore H. (1992), *in MARS*, *UofA Press*. 686-729. [3] Hartmann, W.K. (2001) *Icarus*, 149, 37-53. [4] Golombek M. (2020) *Nat.Com.* 11(1), 1014. [5] Wojcicka, N. et al. (2020) *JGR: Planets* 125(10). [6] Rajšić, A. et al. (2021) *JGR: Planets,* 126(2). (12). [7] Rajšić, A. et al. (2022). *LPI Contributions* 2678, 1335. [8] Posiolova, L.V. et al. (2022) *Science*, 378, 412-417. [9] Gudkova; T. et al. (2015) *EPSL, 427, 57-65.* [10] Bart et al. (2011) *Icarus* 215, 485-490. [11] Warner, N.H. (2017) *Sp. Sci. Rev.* 211, 147-190. [12] Warner, N.H. (2022) *JGR: Planets,* 127, e2022JE007232 [13] Benedix, G.K. et al. (2020) *ESS,* 7(3). [14] Lagain, A. et al. (2021a) *Nat.Com.,* 12, 6352. [15] Lagain, A. et al. (2021b) *ESS*, 8(2). [16] Tanaka, K.L. et al. (2014) *PSS*, 95, 11-24. [17] Anderson, S. L. et al. (2020) *Met. & Planet. Sci.,* 55, 2461-2471. [18] Anderson, S.L. et al. (2022) *AJL*, 930(2), L25. [19] Van Rossum G. (2020) *The Python Lib. Ref., 3.8.2*. Python Software Foundation. [20] Kneissl, T. (2011) *PSS*, 59, 1243-1254. [21] Lagain, A. et al. (2021c) *GSA book, LMI VI.* [22] Michael, G.G. & Neukum, G. (2010) *EPSL* 294, 223-229. [23] Hartmann, W.K. (2005) *Icarus*, 174, 294-320. [24] Melosh, H.J. (1989) *Oxford: Clarendon Press.* [25] Golombek, M (2020), *JGR: Planets,* 125(8) [26] Golombek, M. (2014) *JGR: Planets*, 119, 2522–254. [27] Elliot, J.R. (2022), *Icarus*, 375, 114869.